Introduction to Echocardiography

22

Jamie L. Lohr and Shanthi Sivanandam

Abstract

Advances in ultrasound technology in the last 30 years have allowed transthoracic echocardiography to become the primary technique for noninvasive assessment of cardiac structure and function in patients with congenital and acquired heart disease. Advanced ultrasound techniques, including transesophageal echocardiography and intravascular ultrasound, are widely used and can refine imaging and improve outcomes during invasive cardiac procedures. Better resolution and advanced Doppler techniques have allowed more accurate diagnoses and improved monitoring of pathologic conditions, and provide tools to study embryonic and fetal cardiac development. Finally, ultrasound technologies play an important role in cardiovascular research as well and are currently applied to research in physiology, molecular biology, vascular and cardiac regeneration, and stem cell therapies.

Keywords

Echocardiography • Cardiac ultrasound • Cardiac development • Fetal echocardiography • Doppler • Ejection fraction • Cardiac function

22.1 Introduction

The use of ultrasound to provide noninvasive evaluation of cardiac structure and function was a revolutionary advancement in cardiac care in the late twentieth century [1]. Development of the field of echocardiography has allowed detailed serial examinations of the development, structure, and function of the human heart both in normal physiologic states and in pathologic conditions Echocardiography has increased the diagnostic accuracy of noninvasive cardiac evaluation and provides a tool for the monitoring of diagnostic and therapeutic procedures. The goals of this chapter are to: (1) provide the reader with a brief overview of the types of echocardiography in clinical use today; (2) review the physical principles that underlie this clinical tool; and (3) demonstrate how echocardiography can be used to assess cardiac structure and function.

Prior to the 1970s, diagnosis of congenital and acquired heart disease was achieved by the combination of physical examination, electrocardiography (ECG), and invasive cardiac catheterization. Unfortunately, clinical examination and ECG are often not very specific diagnostic tools. Cardiac catheterization can augment clinical information, but can be a stressful and risky procedure, particularly in the young or very ill patient. Noninvasive imaging, including echocardiography, CT, and MRI, has become the mainstay of cardiac anatomic and functional diagnoses in congenital heart disease.

J.L. Lohr, MD (✉)
Department of Pediatrics, Division of Pediatric Cardiology, University of Minnesota, 2450 Riverside Avenue, MB 560, Minneapolis, MN 55454, USA

Pediatric Cardiology, University of Minnesota Children's Hospital, East Building MB560, 2450 Riverside Avenue, Minneapolis, MN 55454, USA
e-mail: lohrx003@umn.edu

S. Sivanandam, MD
Department of Pediatrics, Division of Pediatric Cardiology, University of Minnesota, 2450 Riverside Avenue, MB 560, Minneapolis, MN 55454, USA

P.A. Iaizzo (ed.), *Handbook of Cardiac Anatomy, Physiology, and Devices*, DOI 10.1007/978-3-319-19464-6_22

Currently, cardiac catheterization is reserved primarily for focused hemodynamic information that compliments noninvasive methods or intervention.

Initial attempts at imaging the heart using reflected sound waves were made in the 1950s, with improvement in the experimental technology and its initial clinical application in the 1960s [1]. During the 1970s, simple motion-mode (M-mode) or linear images were available to define cardiac structures, but these were not adequate for providing great diagnostic detail in complex congenital heart disease. During the 1980s, the technology to provide two-dimensional real-time imaging of the heart was developed, and this subsequently revolutionized noninvasive evaluation of cardiac structure and function. In the late 1980s, techniques of Doppler ultrasound, including color mapping, were developed to extend the analyses of cardiac function and hemodynamics [1]. By the late 1980s, many cardiac defects could be diagnosed accurately and repaired completely without invasive testing. Currently, techniques of echocardiography are being refined to provide more accurate noninvasive assessments of cardiac function in normal and disease states.

22.2 Physical Principles of Echocardiography

22.2.1 Ultrasound Imaging of Tissues

Echocardiography uses the properties of sound waves to differentiate tissues of varied density in the human body. Sound travels in mechanical waves with a speed dependent on the density and the elastic properties of the medium in which they are traveling [2]. This property of tissue is termed its *acoustic density*. Ultrasound waves, which are used in medical applications, have frequencies that are higher than those audible to the human ear. Ultrasound frequencies are generally over 20,000 cycles/s or Hertz, and most cardiac applications are performed using frequencies of two million to ten million Hertz or 2–10 mega Hertz (MHz). When a sound wave, which is generated by electrical stimulation of a piezoelectric crystal, travels through an interface between two tissues of varied acoustic density, such as myocardium and blood, a portion of the energy is reflected backward (the reflected wave) and the rest travels forward through the next tissue (the refracted wave). The reflected wave is received by the transducer, turned back into electrical energy, amplified, and displayed [1]. If there is too much variance between the acoustic density of the tissues being imaged (as in air-filled lung and myocardium or bone and myocardium), the entire ultrasound wave is reflected and the cardiac structures cannot be imaged [1]. The amount of reflected wave detected during ultrasound imaging depends not only on the acoustic characteristics of the interface but also on the angle of incidence or interrogation. An ultrasound beam that encounters a flat surface that is perpendicular to the beam will reflect a wave in the direction of the transmitted sound. In contrast, a beam that is parallel to a structure or that encounters an irregularly shaped structure, as is common in tissue imaging, will be reflected with a degree of scatter that is proportional to the angle of incidence [2].

22.2.2 Resolution of Structures

The ability of cardiac ultrasound to provide anatomical resolution depends on the wavelength of the sound used. The speed of transmission, the frequency, and the wavelength are related by the equation $c = f \times \lambda$ or $\lambda = c/f$, where c = the speed of sound in the medium, f = the frequency of the wave (in Hertz or cycles per second), and λ = the wavelength. Thus, a higher frequency transducer will produce a smaller wavelength and improved resolution along the path of the beam, also termed *axial resolution* [1]. Axial resolution is generally two times the wavelength used, so that a 3.5 MHz transducer has a wavelength of 0.43 mm and an axial resolution of 0.86 mm, while a 7.5 mHz transducer (appropriate for use in pediatric imaging) has a wavelength of 0.2 mm and axial resolution of approximately 0.4 mm [1]. Unfortunately, the use of high-frequency transducers is limited because the smaller wavelengths cannot penetrate as deeply into tissue, and they are therefore less useful for cardiac imaging in adults. Lateral resolution in echocardiography is impacted by the diameter of the beam width, which is a function of the transducer size, shape, and focal plane, as well as the frequency [1].

22.3 Imaging Modalities

22.3.1 M-Mode Echocardiography

M-mode, or motion-mode, echocardiography was the first type of ultrasound used for clinical cardiovascular imaging. Its use today is primarily limited to assessment of valve motion and reliable reproducible measurements of chamber sizes and function [1, 3]. In M-mode echocardiography, a narrow ultrasound beam is pulsed rapidly in a single plane through the heart, and the movements of the structures in that single plane are plotted against time with very high temporal and axial resolution. M-mode echocardiography can be used to assess cardiac wall thickness, aortic root size, chamber sizes, and ventricular function. In general, left ventricular function is quantitated using M-mode by determining the percent of fractional shortening of the left ventricle, which is calculated using the following equation:

$$\mathrm{SF}(\%) = (\mathrm{LVEDD} - \mathrm{LVESD}) / \mathrm{LVEDD} \times 100$$

where SF = shortening fraction, LVEDD = left ventricular end-diastolic dimension, and LVESD = left ventricular

end-systolic dimension. Normal values vary with age and range from 35–45 % in infants to 28–44 % in adolescents and adults [4, 5].

22.3.2 Two-Dimensional Imaging

Two-dimensional imaging provides an arc of imaging planes by employing multiple ultrasound beams to provide cross-sectional views of the heart. Currently, two-dimensional imaging provides the majority of information about cardiac structure and function in routine clinical studies. Two-dimensional imaging requires the presence of multiple beams of ultrasound interrogation in a single transducer, and several types of transducers are available to achieve this. Transducers available for two-dimensional imaging include mechanical (a sweeping or rotating ultrasound beam), phased array (multiple independently controlled sources), and linear array (a line of crystals simultaneously generating a beam of ultrasound). Today, phased array transducers are most commonly used due to their: (1) small size, (2) ability to provide simultaneous two-dimensional and M-mode or Doppler imaging, and (3) improved control of focal length for more uniform images throughout the field of view [6]. In addition to using two-dimensional imaging for viewing anatomic detail, left ventricular function can be quantitated using this mode by estimating left ventricular ejection fractions. This method, which has been shown to correlate well with angiographic estimates of ventricular function, takes advantage of the conical shape of the left ventricle to estimate end-diastolic and end-systolic ventricular volumes from tracings of two-dimensional images using Simpson's biplane rule [3]. The ejection fraction is calculated as follows:

$$\mathrm{EF}(\%) = (\mathrm{LVEDV} - \mathrm{LVESV}) / \mathrm{LVEDV} \times 100$$

where EF = ejection fraction, LVEDV = left ventricular end-diastolic volume, and LVESV = left ventricular end-systolic volume.

Normal values for ejection fractions are approximately 55–65%, and cardiac outputs can be estimated by multiplying the volume ejected with each beat (stroke volume) by the heart rate, using the equation:

$$\mathrm{CO} = \mathrm{HR} \times \mathrm{SV}$$

where CO = cardiac output, HR = heart rate, and SV = stroke volume.

22.3.3 Doppler Ultrasound

The *Doppler Principle*, described by Christian Johann Doppler in 1843, states that the frequency of transmitted sound is altered when the source of the sound is moving [2]. The classic example is the change in pitch of a train whistle as it moves, getting higher as it approaches the receiver and lower as it moves away from it. This change in frequency, or Doppler shift, also occurs when the source of sound is stationary and the waves are reflected off a moving target, including red blood cells in the vasculature. The shift in frequency is related to the velocity of the moving target, as well as the angle of incidence, and is described by the equation:

$$F_{\mathrm{d}} = (2(f_0)(V)\cos\ \phi\ ) / C$$

where F_{d} = observed Doppler frequency shift, f_0 = transmitted frequency, C = velocity of sound in human tissue at 37°C (approximately 1560 m/s), V = blood flow velocity, and ϕ = the intercept angle between the ultrasound beam and the blood flow. Using this principle, Doppler ultrasound can be used to noninvasively estimate the velocity of blood flow in the human heart and vasculature. Using a modified Bernoulli equation where pressure drop is equal to four times the velocity squared (4 V^2), Doppler ultrasound can also be used to estimate chamber pressures and gradients and to provide significant noninvasive hemodynamic data.

22.3.4 Continuous Wave Doppler

Continuous wave Doppler is performed by using a single transducer with two separate elements for transmission and reception of sound waves, so that there is continuous monitoring of the Doppler shift. This technique enables detection of very high-velocity blood flow, but does not allow localization of the site of velocity shift along the line of interrogation [1].

22.3.5 Pulse Wave Doppler

Pulse wave Doppler uses bursts of ultrasound alternating with pauses to detect Doppler shift in a localized region. The timing between the generation of the ultrasound wave and detection of the reflected wave determines the depth of interrogation. Pulse wave Doppler is useful to measure velocity changes in a region defined by two-dimensional echocardiography, however, the spatial resolution limits the velocity shifts detected. In general, the maximal velocity shift detectable is one half of the Doppler sampling rate (pulse repetition frequency or PRF) and is designated the *Nyquist limit* [1]. The maximal sampling rate is determined by the distance of the sampling site from the transducer and the transducer frequency, so that sampling from a transducer position nearer to the region to be interrogated and using a lower frequency transducer will improve the detection and localization of higher velocity flow [1].

22.3.6 Color Doppler Flow Mapping

Color Doppler flow mapping uses the principles of pulsed Doppler to examine multiple points along the scan lines. The mean velocity and direction of these signals are calculated and then displayed and superimposed upon a two-dimensional image. By convention, flow directed toward the transducer is red, and flow directed away from the transducer is blue. Accelerated or turbulent flow is given a different color, typically yellow and green. Color flow mapping is valuable because of the large amount of information that can be obtained in a single image. It can also aid in the: (1) localization of flow accelerations, (2) quantitation of valvar regurgitation, (3) visualization of intracardiac shunting, and/or (4) assessment of arterial connections. Information obtained from color Doppler can be further refined by pulse wave Doppler and continuous wave Doppler interrogation.

22.3.7 Quantification of Pressure Gradients Using Doppler Shift Measurements

Today, quantification of pressure gradients using Doppler echocardiography can provide hemodynamic information that could previously be obtained only by invasive cardiac catheterization. Specifically, the Bernoulli equation [3, 7] defines the relationship between velocity shifts across an obstruction and the pressure gradients caused by the obstruction. For practical purposes, the proximal velocity is neglected and the simplified equation becomes: pressure difference = distal velocity squared × 4. This is a valuable way to estimate pressure drops across obstructive valves and/or pressure differences between chambers (based on the velocities of valvar regurgitation or intracardiac shunting).

22.3.8 Myocardial Performance Index

The *myocardial performance index* (MPI) is a noninvasive Doppler measurement of global) ventricular function that incorporates both systolic and diastolic function and may be applied to the right ventricle (RV) or left ventricle (LV) [8]. The MPI (or Tei index) is defined as a ratio of the sum of the isovolumic contraction time (IVCT) and isovolumic relaxation time (IVRT) divided by the systolic ejection time (ET) (Fig. 22.1). The index is easily measured with high reproducibility and is important in the assessment of global performance, as the active energy cycles of contraction and relaxation occur during IVCT and IVRT. The Tei index is independent of heart rate and blood pressure and can be a useful tool to evaluate myocardial function in different clinical situations [8].

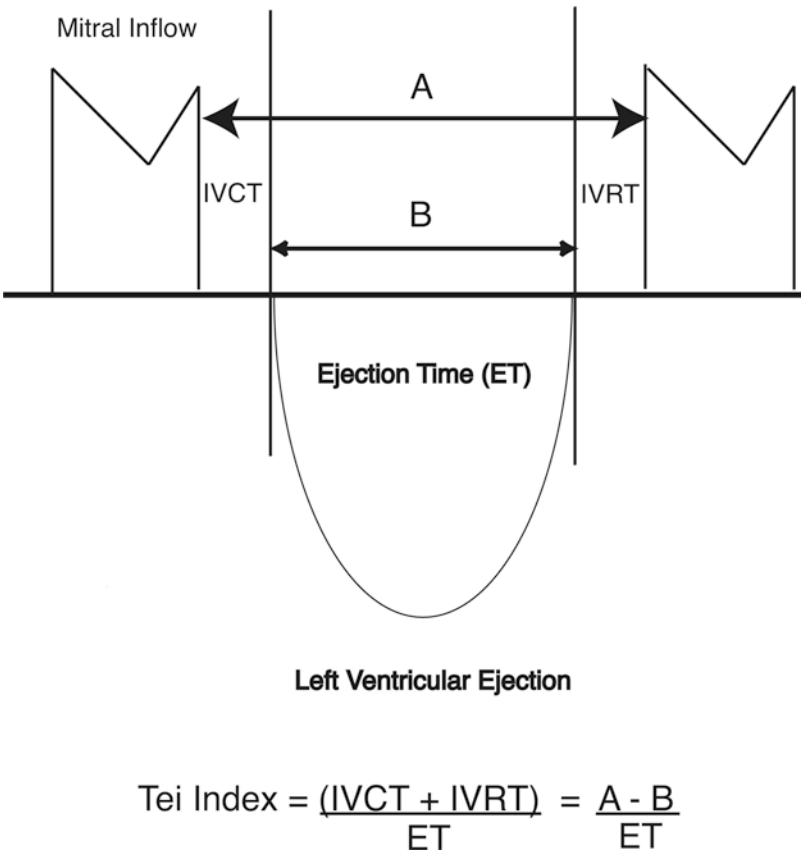

Fig. 22.1 Diagrammatic representation of the myocardial performance index or Tei index. The Tei index is the sum of the isovolumetric contraction time (IVCT) and isovolumetric relaxation time (IVRT) divided by the ejection time (ET). Adapted from Pellet et al. [8]

22.3.9 Tricuspid Annular Plane Systolic Excursion

The *tricuspid annular plane systolic excursion* (TAPSE) can be used to estimate the right) ventricular global systolic function. TAPSE is an easily obtainable, simple, and generally reliable measure of right ventricular ejection fraction, which allows it to be used routinely in clinical studies. TAPSE is defined as the distance traveled by the tricuspid annulus along the direction of the line joining the tricuspid annulus and right ventricular apex at end-diastole. TAPSE assumes that the displacement of the basal and adjacent segments of the RV are representative of the longitudinal function of the entire right ventricle and that longitudinal myocardial shortening is a significant contributor to overall right ventricular function. TAPSE is assessed with M-mode echocardiography oriented on a two-dimensional image in an apical four-chamber view, placing the M-mode cursor on the lateral tricuspid annulus (Fig. 22.2). The annular plane is identified as the first continuous line immediately below the RV cavity (which appears "above" the RV cavity on apical images). Maximum systolic excursion of the lateral annulus is measured and compared to normal values (Fig. 22.2).

22.3.10 Tissue Doppler Imaging

Tissue Doppler imaging (TDI) is an extension of conventional Doppler flow echocardiography that measures myocardial motion and velocity [9] (Fig. 22.3A). Myocardial velocity information can be displayed as a pulse tissue Doppler signal and data color-coded and displayed in real time. Color Doppler allows for visual semi-quantitation of myocardial motion superimposed on conventional M-mode and two-dimensional images. Velocity data from a region of interest can be arranged to obtain spectral displays of tissue velocities. The graphic display includes one positive systolic (S) deflection and two negative diastolic waveforms. The systolic waveform is preceded by regional isovolumic contraction time (RIVCT), and the diastolic waves are preceded by regional isovolumic relaxation time (RIVRT). The first diastolic deflection represents the early rapid filling phase of diastole (E), which is followed by a period of diastasis, and a second late active filling phase of diastole (A) due to atrial contraction (Fig. 22.3B).

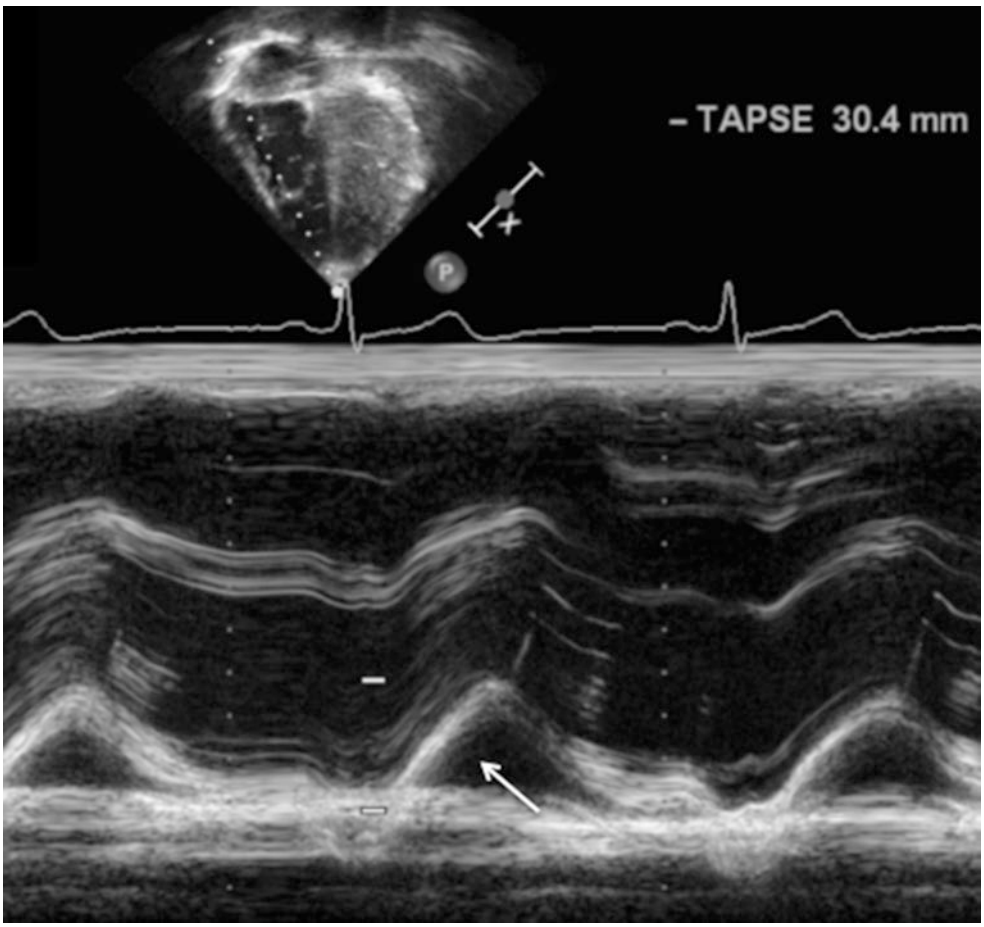

Fig. 22.2 Measurement of the tricuspid annular plane systolic excursion (TAPSE). TAPSE measures the motion of the lateral tricuspid valve annulus (*white arrow*) as it moves toward the RV apex during systole. Normal values are greater than 16 mm and reflect longitudinal shortening as a measure of global RV function

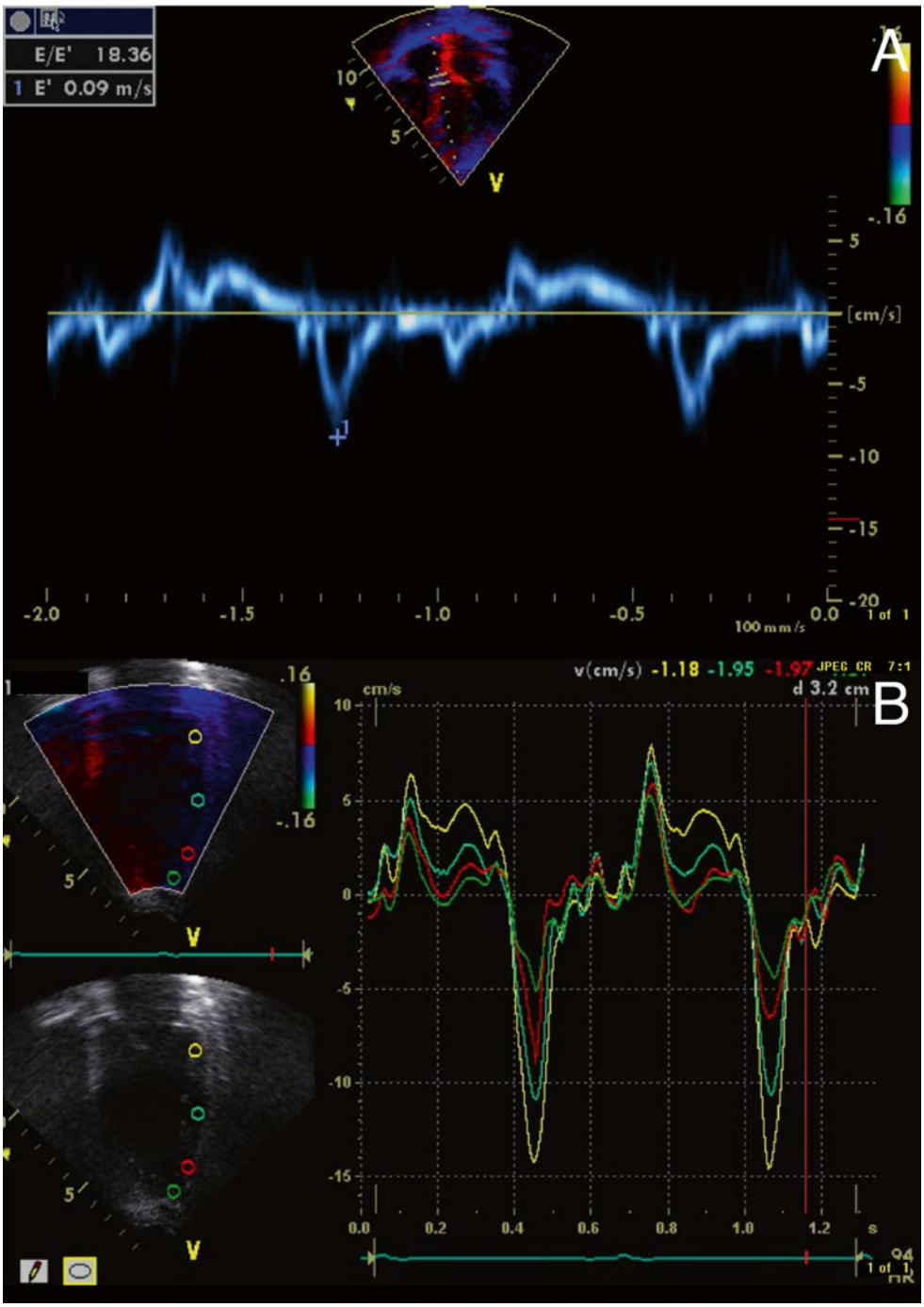

Fig. 22.3 Tissue Doppler imaging. (A) Pulse wave tissue Doppler provides a spectral display of peak tissue velocity. (B) Tissue Doppler velocity data for the quantification of asynchrony from apical four-chamber view. Sample volumes are in the lateral septal segment

22.4 Clinical Applications of Cardiac Ultrasound

22.4.1 Transvaginal and Transabdominal Fetal Echocardiography

The human fetal heart is fully developed and functional by 11 weeks after conception. Using transvaginal ultrasound, the structure and functional characteristics of the fetal heart can be observed as early as 9 weeks of gestational age [10]. This technique remains the most useful type of fetal cardiac imaging until approximately 16 weeks of gestation. At that time, transabdominal imaging becomes the preferred method (Fig. 22.4). Fetal imaging is routinely performed at 16–20 weeks of gestational age, and image quality improves until about 24–28 weeks of gestational age [10]. The quality of fetal images can be reduced by loss of amniotic fluid, maternal body habitus, fetal bone density, and/or the fetal position. M-mode, two-dimensional, and Doppler ultra-

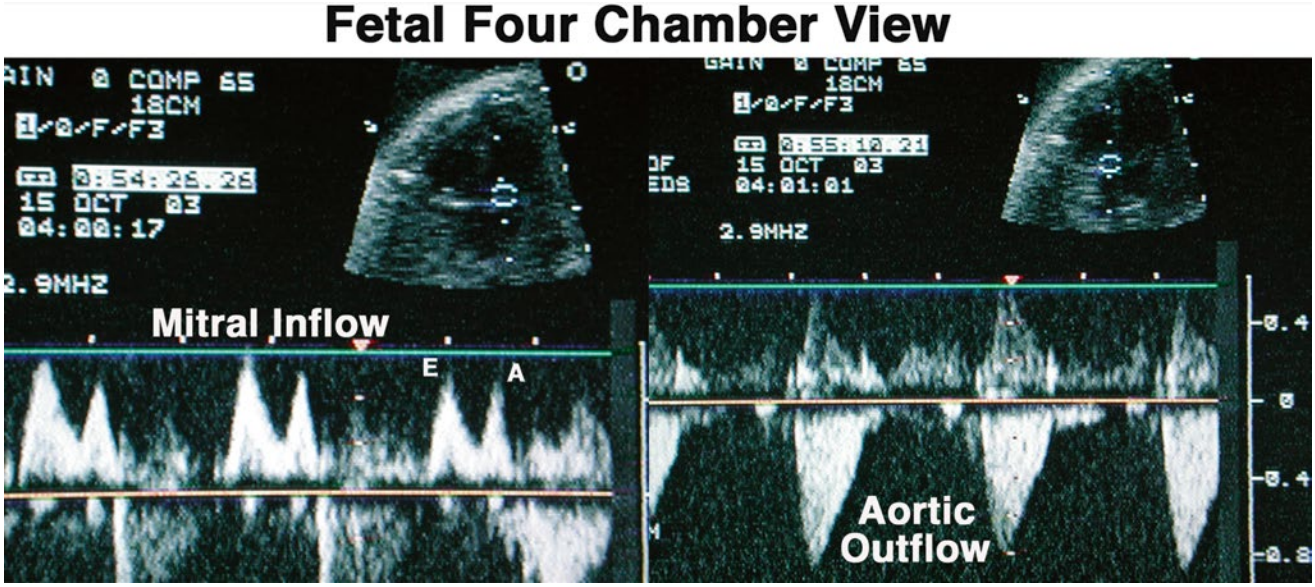

Fig. 22.4 Fetal echocardiogram at approximately 24 weeks gestation. Four-chamber views are shown with pulse wave Doppler analysis of mitral inflow and aortic outflow. Mitral inflow is characterized by two waves, an E wave representing passive filling of the left ventricle in diastole and an A wave representing active filling of the ventricle with atrial systole. Doppler flows are less than 1 m/s (indicating unobstructed blood flow), and the interval between aortic outflow signals is approximately 0.5 s (indicating a fetal heart rate of 120 beats/min)

sound techniques are useful for analyses of the anatomy and function of the fetal heart, the diagnoses and monitoring of fetal arrhythmias, and the guidance of fetal interventional procedures. In general, fetal echocardiography has contributed to: (1) improved understanding of the natural history of many forms of congenital heart disease; (2) improved monitoring and obstetric care of fetuses with structural heart diseases and arrhythmias; and (3) attempts at in utero correction of vascular, valvular, and structural cardiac abnormalities [11, 12].

22.4.2 Transesophageal Echocardiography

Transesophageal echocardiography allows imaging of the heart from the esophagus or stomach, which improves image resolution by eliminating much of the acoustic interference from the lungs and chest wall while, at the same time, allowing for reduced distance of the ultrasound source to the heart. Transesophageal imaging is performed using either a biplane probe (two single plane arrays set at perpendicular planes) or a rotating single array probe that provides multiple planes of view (an omniplane probe). Today, transesophageal probes come in sizes appropriate for use in adults, children, and infants. Transesophageal echocardiography is used when improved resolution is required or when transthoracic windows are unavailable, as is typical in the operating room or cardiac catheterization laboratory [3]. It also has become a routine form of intraoperative monitoring for open-heart surgery and is specifically useful to detect incomplete repairs prior to separation from cardiopulmonary bypass [13]. It is also a useful adjunct to interventional cardiac catheterization procedures. Transesophageal echocardiography typically requires sedation or anesthesia and thus adequate patient monitoring. Note that it is significantly more invasive than standard transthoracic echocardiography and can be complicated by airway compromise, dysphagia, or esophageal perforation [3, 14, 15].

22.4.3 Transthoracic Echocardiography

Today, *transthoracic echocardiography* remains as the most common method for cardiac imaging. It is noninvasive, can be performed in any cooperative patient, and only rarely requires sedation. Yet, images obtained are limited by patient size and can be complicated by interference from soft tissues, bone, or lung. The transthoracic echocardiogram is performed from standard windows on the chest (Fig. 22.5) and requires the use of multiple transducers at varied ultrasound frequencies to maximize the two-dimensional image resolution and Doppler ultrasound information obtained. Most commonly, images are obtained by trained and licensed cardiac sonographers and then interpreted by a cardiologist.

22.4.4 Standard Transthoracic Examination

Currently, the *standard transthoracic cardiac echo* includes images from parasternal, apical, suprasternal notch, and subcostal imaging windows (Fig. 22.5). Two-dimensional sec-

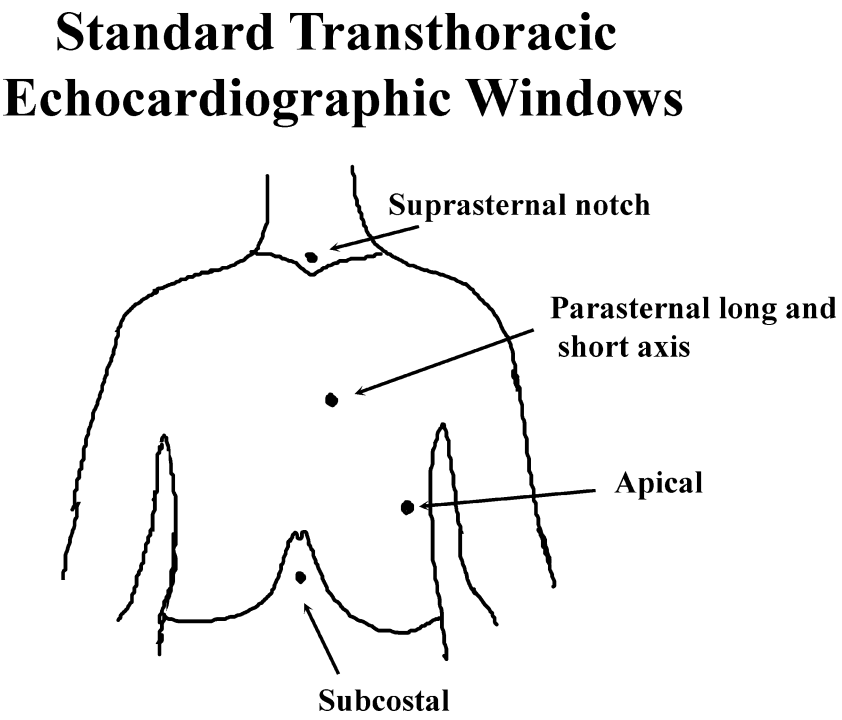

Fig. 22.5 Diagram of the chest showing transducer position for standard transthoracic echocardiographic windows. A typical examination in a cooperative patient is performed in a standard order: parasternal, apical, subcostal, and then suprasternal notch views. Perpendicular imaging planes can be obtained from each position by rotating the transducer 90°

tors are imaged in each window to provide anatomic details and functional analyses. The highest frequency transducer set at the lowest depth possible is used to maximize image resolution while scanning for anatomical detail. Two-dimensional images are then used to guide Doppler ultrasound interrogations, often with a lower frequency transducer that will optimize Doppler information. Two-dimensional images are also used to guide M-mode measurements of chamber size and function, and Doppler gradients are calculated across valves and shunts to maximize the hemodynamic information obtained.

The standardized transthoracic echocardiograms are obtained by scanning at four regions on the chest wall: the parasternal window, apical window, subcostal region, and suprasternal notch (Fig. 22.5). Parasternal long-axis views are used to obtain *long-axis* images of the left side of the heart, including the left atrium, left ventricle, and aorta (Fig. 22.6). A subtle tilt of the transducer inferiorly from this position gives views of the right atrium, tricuspid valve, and right ventricle, and tilting leftward brings the pulmonary valve and main pulmonary artery into view. Turning the transducer and scan plane by 90° results in short-axis views of the heart in planes from the base of the heart (region of the aorta, tricuspid, and pulmonary valves) to the apex (Fig. 22.7A–D). M-mode measurements of the left-sided chambers are obtained from parasternal short-axis windows and can be used to assess chamber size and function (Fig. 22.7E, F). Apical windows reveal standard four-chamber views of the left atrium, mitral valve, left ventricle, right atrium, tricuspid valve, and right ventricle (Fig. 22.8A, B). This view sends the ultrasound beam parallel to the septal structures, so is not adequate to assess the integrity of the atrial or ventricular septums. Tilting the transducer anteriorly results in a five-chamber view that allows excellent visualization of the left ventricular outflow tract and aorta. Doppler gradients across the mitral, tricuspid, and aortic valves can also be obtained from this view (Fig. 22.8C), and the velocity of tricuspid valve regurgitations can be used to estimate right ventricular and pulmonary artery systolic pressures.

Subcostal views are particularly useful in patients with lung disease or in those who have had recent open-heart surgery. From subcostal images, the orientation of the heart in the chest and the major vascular connections can be established. Subcostal views also provide excellent visualization of the intra-atrial septum (Fig. 22.9A) and four-chamber views in patients with poor apical windows. Suprasternal notch views are most useful for visualization of the aortic arch, its branching vessels, and the descending thoracic aorta (Fig. 22.9C), as well as for determining the Doppler shifts across the aortic valve. This view is also important to exclude vascular abnormalities, including coarctation of the aorta.

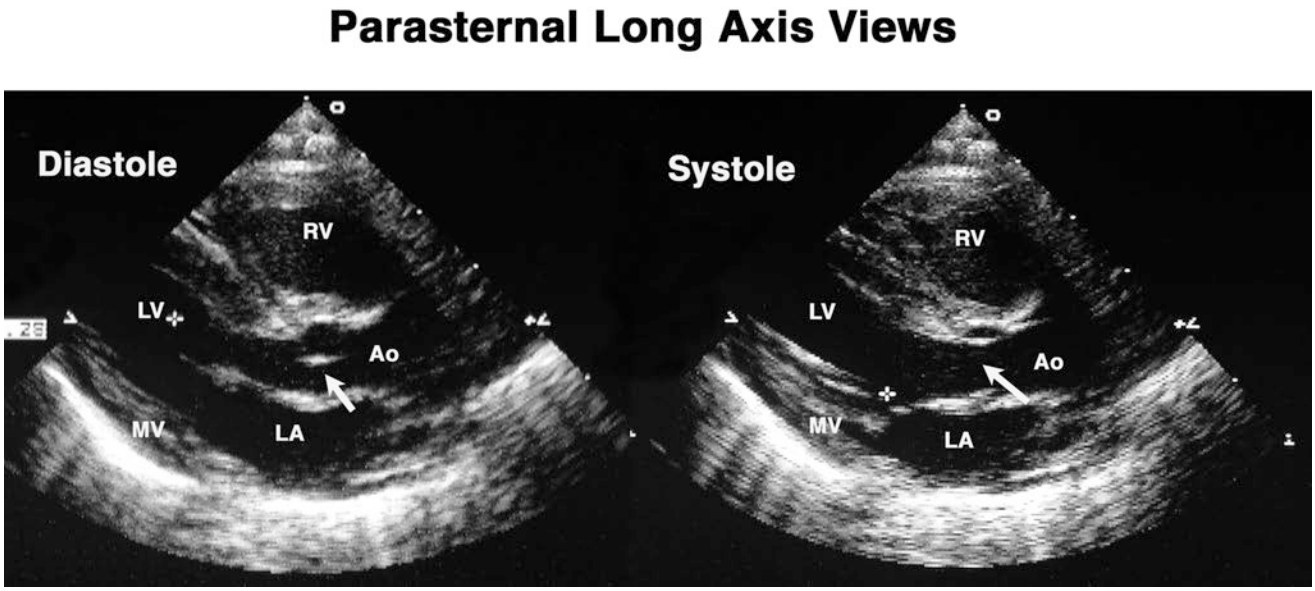

Fig. 22.6 Transthoracic parasternal long-axis views in a newborn infant. These views demonstrate the long axis of the left side of the heart. Frame 1 is in diastole with an open mitral valve to accommodate left ventricular filling and a closed aortic valve (*arrow*). Frame 2 is in systole with an open aortic valve (*arrow*) and closed mitral valve (*asterisk*). *White dots* on the sector border represent centimeter marks. *Ao* aorta, *LA* left atrium, *LV* left ventricle, *RV* right ventricle, *MV* mitral valve

22.5 Other Techniques in Cardiac Ultrasound

The use of ultrasound for cardiac imaging and investigation of hemodynamics has been revolutionary in the diagnoses and treatment of heart disease. Currently, ultrasound techniques available for use on a limited clinical basis include intravascular ultrasound (IVUS) and three- and four-dimensional imaging. Research applications of cardiac ultrasound include embryonic and small animal cardiac imaging. IVUS uses catheters with ultrasound transducers mounted on the tips. These transducers are capable of cross-sectional imaging or true sector imaging using phased array ultrasound transducers mounted on their tips [3, 16]. As technology has improved, relatively small catheters (5 and 6 French) and high-frequency transducers (40–45 MHz) are available for the imaging of the aorta and pulmonary arteries, aortic and pulmonary valves, and/or coronary arteries [17]. Coronary artery imaging has been particularly useful in heart transplant patients as a means to detect intimal thickening associated with chronic rejection [18] and in patients with Kawasaki syndrome who commonly develop coronary artery aneurysms [3]. IVUS has also been used for intracardiac monitoring of interventional procedures [16] and has recently been shown to reduce rates of stent thrombosis and adverse cardiac events in drug-eluting stents [17, 19]. Lead extraction procedures are also aided by the use of IVUS.

Three-dimensional imaging technology has recently been improved so that cardiac images can be displayed in real time (four-dimensional imaging). Three- and four-dimensional images are useful for the re-creation of a movable three-dimensional image to assist with surgical planning [1]. Unfortunately, currently large transducer sizes and slow image processing capabilities make three- and four-dimensional imaging less desirable for routine cardiac ultrasound examinations [7]. Ultrasound imaging technology has been improved so that the heart can be studied during embryonic development. For example, pregnant mice can be anesthetized and undergo fetal cardiac imaging as early as 8–9 days after conception, so that the anatomy and blood flow patterns can be observed during both normal and abnormal cardiac development [2, 20, 21]. Additionally, ultrasound techniques can be applied to vertebrate and nonmammalian model systems to study physiology, cardiac regeneration, and cell therapies [22–25].

22.6 Summary

The development and application of clinical echocardiography has enabled thorough, accurate, and noninvasive evaluations of both cardiac structure and function. Today, transthoracic echocardiography remains as the mainstay of cardiac diagnosis and monitoring in both adult and pediatric

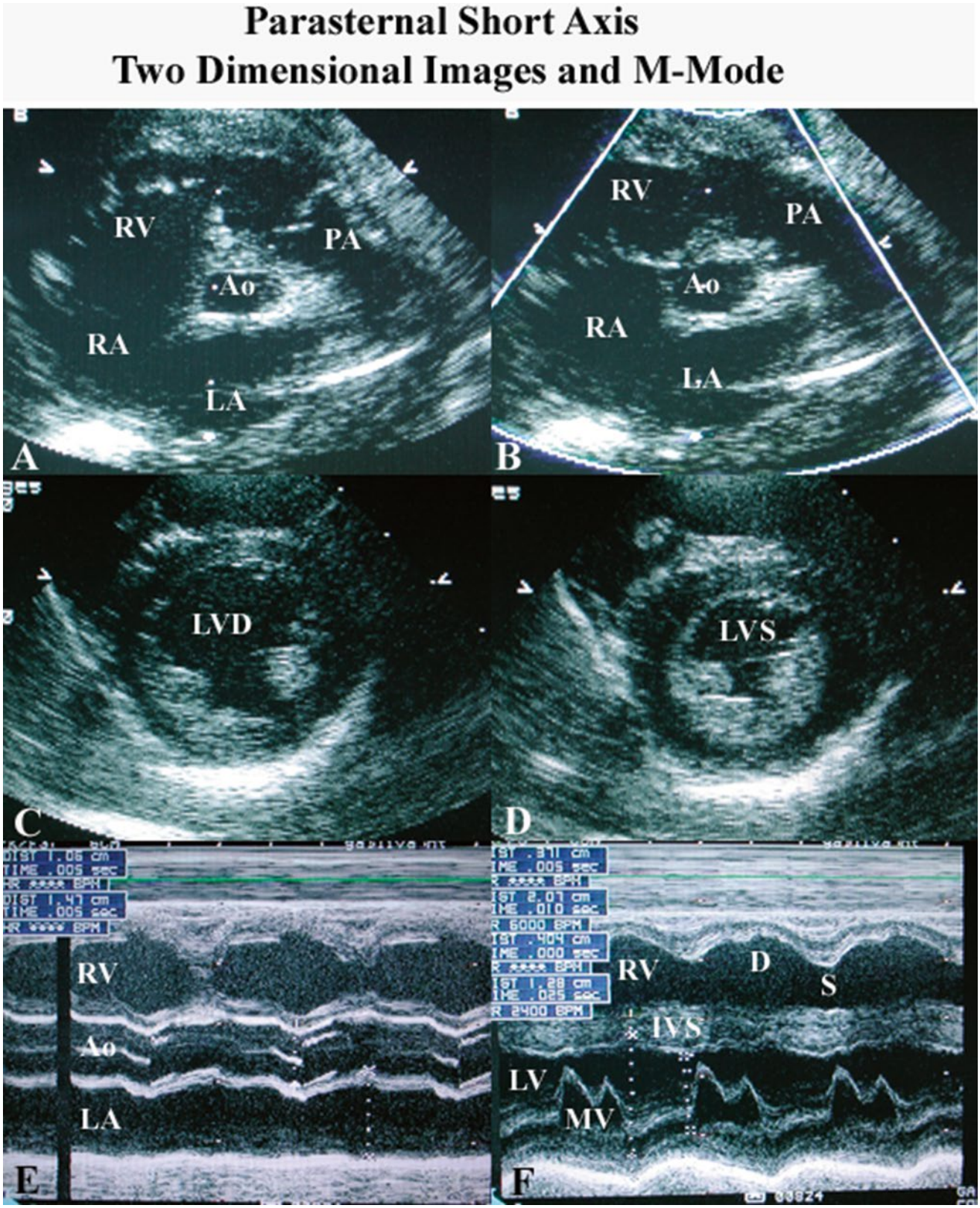

Fig. 22.7 Two-dimensional and M-mode images obtained from parasternal short-axis views. Panel A shows a view through the base of the heart in diastole. Panel B shows the same imaging plane in systole, with the pulmonary valve open. M-mode measurements of the right ventricle, aorta, and left atrium (Panel E) are obtained in this plane. Panel C demonstrates a cross-sectional or short-axis view of the left ventricle at the level of the papillary muscles in diastole, and Panel D is at the same plane in systole. This is the appropriate level for quantification of left ventricular function by shortening fraction. Panel F shows an M-mode recording at the level of the mitral valve, a plane just above that seen in Panels C and D. Abnormalities of mitral valve motion can be demonstrated in this plane. *LA* left atrium, *RA* right atrium, *RV* right ventricle, *Ao* aorta, *PA* main pulmonary artery, *LVD* left ventricle, diastole, *LVS* left ventricle, systole, *D* diastole, *S* systole, *IVS* interventricular septum

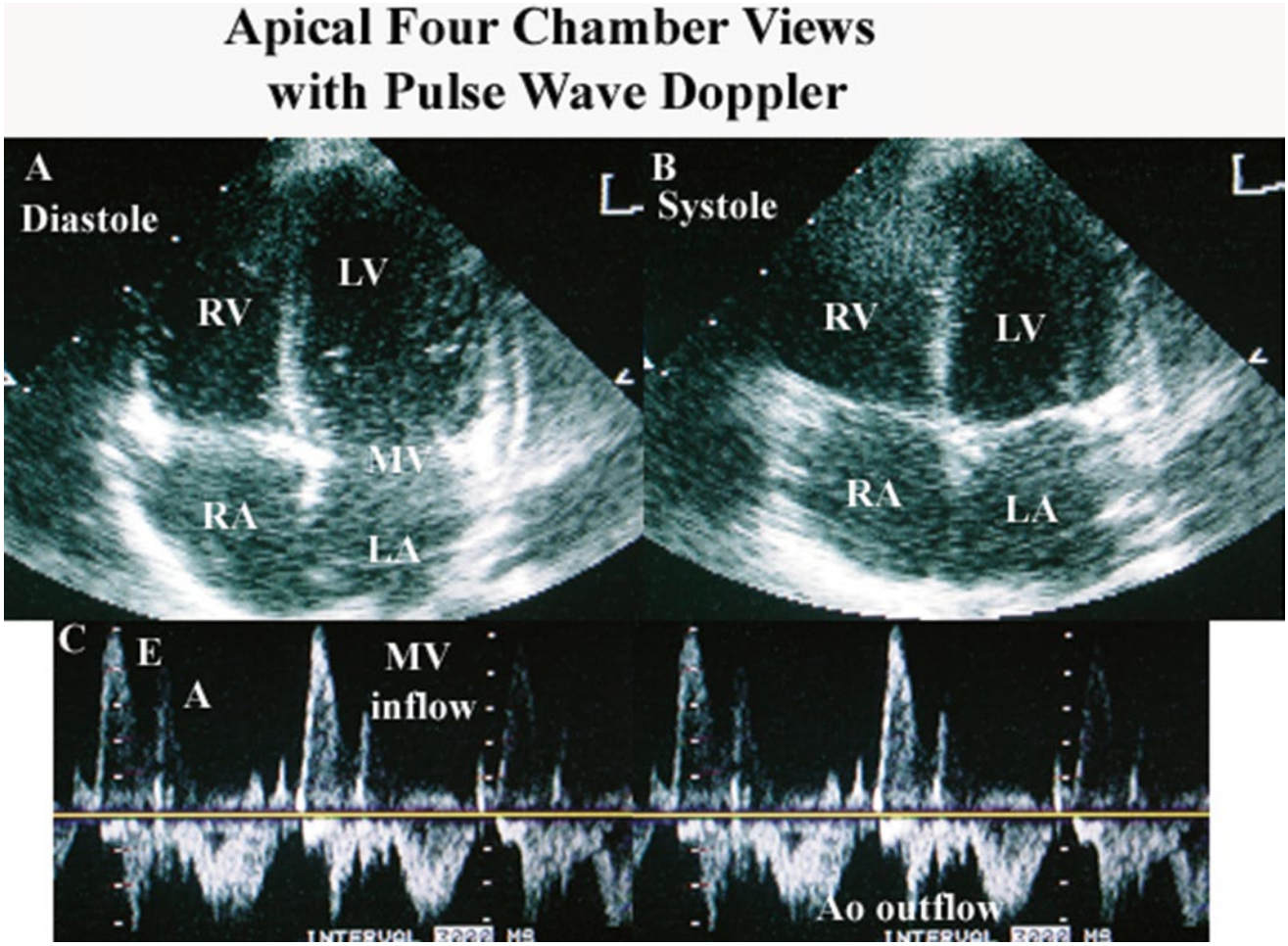

Fig. 22.8 Panel A is a two-dimensional apical four-chamber views of the heart in diastole (open mitral valve), and Panel B shows the same imaging plane in systole (closed atrioventricular valves). The pulsed wave Doppler tracing shown in Panel C demonstrates mitral inflow toward the transducer (above the baseline) and aortic outflow away from the transducer (below the baseline). The mitral valve inflow tracing shows passive filling of the left ventricle during early diastole (E) followed by active filling of the left ventricle in late diastole with the onset of atrial contraction (A). Aortic outflow occurs in systole. *LA* left atrium, *RA* right atrium, *RV* right ventricle, *LV* left ventricle, *MV* mitral valve

patients. Advances in two-dimensional imaging allow significant anatomic detail to be visualized, especially in smaller patients, and Doppler ultrasound allows for direct visualization of altered flow patterns and noninvasive investigations of hemodynamics. New Doppler methods have improved the quantification of regional and diastolic myocardial function. The use of transesophageal echocardiography, although slightly more invasive, has also become routine when improved resolutions and/or intraprocedural monitoring are required. Future directions in echocardiography include: (1) increased utilization of IVUS for diagnoses and monitoring of interventional procedures; (2) improvements in three-dimensional ultrasound techniques that will make them appropriate for routine imaging; and (3) the use of embryonic imaging to study normal and abnormal heart development.

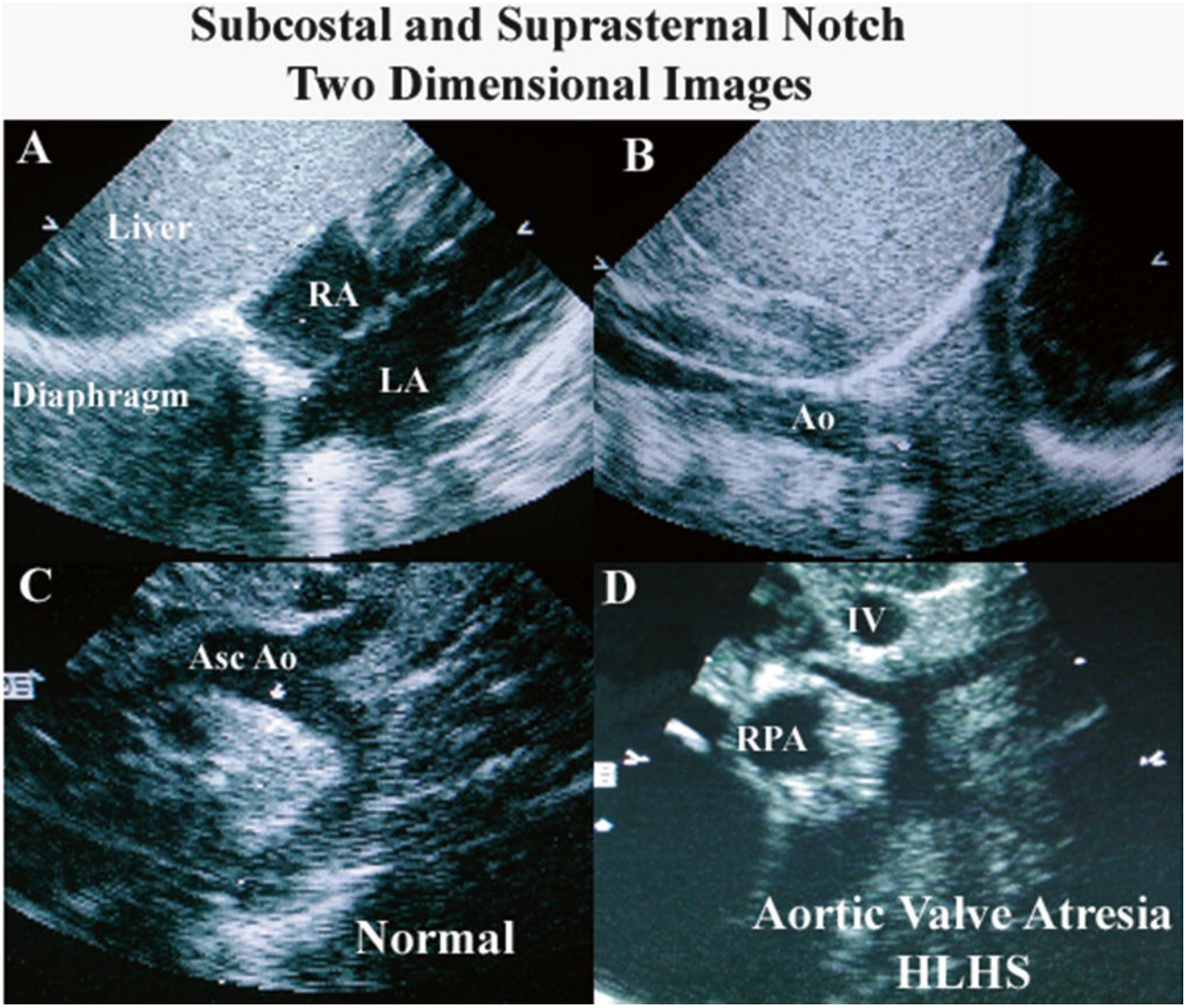

Fig. 22.9 Two-dimensional images from subcostal windows (A, B) and suprasternal notch windows (C, D). Subcostal views provide orientation of the heart relative to the abdominal organs as in Panel A, which shows a rightward liver and leftward cardiac apex. Subcostal windows also provide excellent four-chamber views as well as short-axis views of the interatrial septum in smaller individuals, as shown in Panel A. Panel B is a subcostal view showing the descending thoracic aorta at the level of the diaphragm. Panel C is a suprasternal notch view of a normal aortic arch. Panel D shows the severe hypoplasia of the ascending aorta seen in a patient with hypoplastic left heart syndrome (HLHS) caused by aortic atresia. *LA* left atrium, *RA* right atrium, *Ao* aorta, *AscAo* ascending aorta, *RPA* right pulmonary artery, *IV* innominate vein

Acknowledgments The author would like to thank Jim Berry, Kim Berry, and Jay Hall for providing the images shown in this chapter and Kim Berry and Jay Hall for the review of this manuscript.

References

1. Geva T (1998) Echocardiography and Doppler ultrasound. In: Garson A Jr (ed) The science and practice of pediatric cardiology. Williams and Wilkins, Philadelphia, pp 789–843
2. Vermilion RP (1997) Basic physical principles. In: Snider R (ed) Echocardiography in pediatric heart disease. Mosby-Year Book, St. Louis, pp 1–10
3. Snider R, Serwer G, Ritter S (eds) (1997) Echocardiography in pediatric heart disease. Mosby-Year Book, St. Louis
4. Colan SD, Parness IA, Spevak PJ (1992) Developmental modulation of myocardial mechanics: age and growth related alterations in afterload and contractility. J Am Coll Cardiol 19:619–629
5. Gutgessel HP, Paquet M, Duff DF, McNamara DG (1977) Evaluation of left ventricular size and function by echocardiography: results in normal children. Circulation 56:457–462
6. Vermilion RP (1997) Technology and instrumentation. In: Snider R (ed) Echocardiography in pediatric heart disease. Mosby-Year Book, St. Louis, pp 11–21
7. Danford DA, Murphy DJ Jr (1998) Basic foundations of echocardiography and Doppler ultrasound. In: Garson A Jr (ed) The science and practice of pediatric cardiology. Williams and Wilkins, Philadelphia, pp 539–558

8. Pellet AA, Tolar WG, Merwin DG, Kerut EK (2004) The Tei index: methodology and disease state values. Echocardiography 21:669–672
9. Knebel F, Reibis RK, Bondke HJ et al (2004) Tissue Doppler echocardiography and biventricular pacing in heart failure: patient selection, procedural guidance, follow-up, quantification of success. Cardiovasc Ultrasound 2:17
10. Allan L (2000) The normal fetal heart. In: Allan L (ed) Textbook of fetal cardiology. Greenwich Medical Media Limited, London, pp 55–91
11. Freud LR, McElhinney DB, Marshall AC et al (2014) Fetal aortic valvuloplasty for evolving hypoplastic left heart syndrome: postnatal outcomes of the first 100 patients. Circulation 130:638–645
12. Allan LD (2012) Rationale for and current status of prenatal cardiac intervention. Early Hum Dev 88:287–290
13. Randolph GR, Hagler DJ, Connolly HM et al (2002) Intraoperative transesophageal echocardiography during surgery for congenital heart defects. J Thorac Cardiovasc Surg 124:1176–1182
14. Stevenson JG (1999) Incidence of complications in pediatric transesophageal echocardiography: experience in 1650 cases. J Am Soc Echocardiogr 12:527–532
15. Rousou JA, Tighe DA, Garb JL et al (2000) Risk of dysphagia after transesophageal echocardiography during cardiac operations. Ann Thorac Surg 69:486–489
16. Ziada KM, Tuzcu EM, Nissen SE (1999) Application of intravascular ultrasound imaging in understanding and guiding percutaneous therapy for atherosclerotic coronary disease. Cardiol Rev 7:289–300
17. McDaniel MC, Eshtehardi P, Sawaya FJ et al (2011) Contemporary clinical applications of coronary intravascular ultrasound. JACC Cardiovasc Interv 4:115511–115567
18. Costello JM, Wax D, Binns HJ et al (2003) A comparison of intravascular ultrasound with coronary angiography for evaluation of transplant coronary artery disease in pediatric heart transplant recipients. J Heart Lung Transplant 22:44–49
19. Witzenbichler B, Maehara A, Weisz G et al (2014) Relationship between intravascular ultrasound and clinical outcomes after drug-eluting stents: the assessment of dual-antiplatelet therapy with drug-eluting stents (ADAPT-DES) study. Circulation 129:463–470
20. Srinivasan S, Baldwin HS, Aristizabal O, Kwee L, Labow M, Turnbull DH (1998) Noninvasive, in utero imaging of mouse embryonic heart development with 40-MHz echocardiography. Circulation 98:912–918
21. Zhou YQ, Foster FS, Qu DW, Zhang M, Harasiewic KA, Adamson SL (2002) Applications for multifrequency ultrasound biomicroscopy in mice from implantation to adulthood. Physiol Genomics 10:113–126
22. Insight through In Vivo Imaging, Vevo 660 System Product Information, Visualsonics (Canada). www.visualsonics.com. Accessed 21 Nov 2014
23. Bartlett HL, Escalera RB 2nd, Patel SS et al (2010) Echocardiographic assessment of cardiac morphology and function in Xenopus. Comp Med 60:107–113
24. Porello ER, Mahmoud AI, Simpson E et al (2011) Transient regenerative potential of the neonatal mouse heart. Science 331:1078–1080
25. Silva GV, Litovsky S, Assad JAR et al (2005) Mesenchymal stem cells differentiated into an endothelial phenotype, enhance vascular density, and improve heart function in a canine chronic ischemia model. Circulation 111:150–156